1 **The dynamical role of upper layer salinity in the Mediterranean Sea**

2 Ali Aydogdu[1], Pietro Miraglio[1], Romain Escudier[2], Emanuela Clementi[1], Simona Masina[1]

3 [1] Ocean Modeling and Data Assimilation Division, Fondazione Centro Euro-Mediterraneo sui Cambiamenti Climatici,

4 Bologna, Italy

5 [2] Observations pour Les Systèmes D'analyse et de Prévision, Mercator Ocean International, Toulouse, France

6 *Correspondence to*: Ali Aydogdu (ali.aydogdu@cmcc.it)

7 **Abstract.**

8 The Mediterranean Sea is a semi-enclosed basin with an excess amount of evaporation compared to the water in-flux through

9 precipitation at the surface and river runoff on the land boundaries. The deficit in the water budget is balanced by the inflow

10 in the Gibraltar Strait and Turkish Straits System connecting the Mediterranean with the less saline Atlantic Ocean and the

11 Black Sea, respectively. There is evidence that the Mediterranean region is a hotspot in a warming climate which will possibly

12 change the water cycle significantly, but with large uncertainties. Therefore, it is inevitable to monitor the evolution of the

13 essential ocean variables to respond to the associated risks and mitigate the related problems. In this work, we evaluate the

14 evolution of the salinity content and anomaly between 0-300 m in the Mediterranean Sea during the last decades using the

15 Copernicus Marine Service reanalysis and in-situ objective analysis products. The results show an increasing mean salinity

16 with a stronger trend in the eastern basin. The spread of the products implies a larger variability in the western basin while

17 the standard deviation is lower in the eastern side, especially in the Ionian and the Levantine basins.

18

19 **Short summary.**

20 This paper investigates the salinity content and anomaly evolution in the Mediterranean Sea using observational and

21 reanalysis products. The salinity content increases overall while negative salinity anomalies appear in the western basin

22 especially around the upwelling regions. There is a large spread in the salinity estimates that reduces with the emergence of

23 the Argo era.

24 **1 Introduction**

25 The Mediterranean Sea is warming (Pisano et al., 2020). It is evaporating more and more (Skliris et al., 2018; Jordà et al.,

26 2017) with marine heat waves increasing in intensity, duration and frequency (Juza et al., 2022; Dayan et al., 2022). The

27 Mediterranean region is a hotspot with global warming (Tuel and El Tahir, 2020) that will likely alter the water cycle (Cos

28 et al., 2022). Tracking the changes of the essential ocean variables (EOVs) is crucial in order to understand the impact of

29 climate change. Two of these EOVs are linked to the ocean salinity at the surface and subsurface, which will be affected

30 significantly by the surface heat and freshwater fluxes. The global water cycle modulating the ocean salinity is a key element

31 of the Earth's climate (Cheng et al., 2020). In the Mediterranean Sea, freshwater fluxes through the land (rivers) and

32 atmosphere (evaporation and precipitation) are balanced by two sea straits, namely Gibraltar and Dardanelles, from which

33 the less saline Atlantic Ocean and Black Sea waters flow into the basin with an annual net inflow of 0.78 ± 0.05 Sv (Soto-

34 Navarro et al., 2010) and 0.05 ± 0.04 Sv (Jarosz et al., 2013), respectively. These density contrasts contribute to the wind

35 driven circulation and generate a highly energetic anti-estuarine circulation (Cessi et al., 2014). The salinity of the Atlantic

36 water entering through the Gibraltar Strait is about 36.2 psu. The salinity of the Dardanelles can vary significantly and it can

37 be as low as 27 psu (Aydogdu et al., 2018; Sannino et al., 2017). Recently, Fedele et al. (2022) studied the characterization

38 of the Atlantic Waters (AW) and Levantine intermediate waters (LIW) from the ARGO profiles in the last 20 years. Their

39 conclusion is a clear salinification and warming trend which characterised both AW and LIW over the last two decades.

40 Skliris et al. (2018) argue that the Mediterranean basin salinification is driven by changes in the regional water cycle rather

41 than by changes in salt transports at the straits, as it is shown by the water mass transformation distribution in salinity

42 coordinates. However, we will show that there is a bigger uncertainty compared to most of the basin in the radius of influence

43 of both the Gibraltar and Dardanelles Straits. In Section 2, the data and methods used in this study are presented. In Section

44 3, the results are shown and discussed, while in Section 4 the conclusions are drawn.

45 **2 Data and method**

46 In this study, Copernicus Marine Service global and regional reanalysis as well as observational gridded products are used to

47 explore the role of the salinity variability in the 0-300 m depth among different estimates as well as temporal and spatial

48 anomalies against a mean.

49 The Mediterranean 1/24° resolution regional reanalysis (hereinafter, MEDREA24; Escudier et al., 2021) from Copernicus

50 Marine Service is used as a regional high-resolution product. In this work, MEDREA24 and its interim extension until the

51 end of 2021 are included. Moreover, the 1/4° resolution Global Reanalysis Ensemble Product (hereinafter, GREP) is also

52 used. It consists of the global reanalysis from Mercator Ocean's GLORYS2V4 (Lellouche et al., 2013), UK MetOffice's

53 GLOSEA5v13 (MacLachlan et al., 2014) using the FOAM system (Blockley et al., 2014), CMCC C-GLORSv7 (Storto et

54 al., 2016) and ECMWF's ORAS5 (Zuo et al., 2017). A study on the ocean heat content and steric sea level representation in

55 the GREP ensemble can be found in Storto et al. (2019a). A more general status of the global ocean reanalysis is reviewed

56 in Storto et al. (2019b). The period covered by the GREP is 1993-2019.

57 As observational products, the CORA (Szekely et al., 2019) and ARMOR3D (Guinehut et al., 2012) gridded reconstructions

58 are adopted. Both datasets are available between 1993 and 2020. In the CORA, the objective analysis is performed on

59 measurement's anomalies relative to a background, at the 15th day of each month while in the ARMOR3D the first guess is
60 adopted from World Ocean Atlas 2018. Both products use an objective analysis method proposed by Bretherton et al., (1976).

61 The investigation is performed in the entire Mediterranean Sea as well as in the eastern and western basins, which have very
62 different characteristics. The salinity mean ($\overline{S}$) is computed using formula (1) as the monthly volume (V) average of each
63 product between 0 and 300 m depth, i.e., excluding the shelf areas close to the coast with a depth less than 300 m.

$$\overline{S} = \frac{1}{V} \int_V S dV$$

64 (1)

66 The mean of different products and their standard deviation are evaluated in the common period 1993-2019. Besides this
67 time frame, the CORA and ARMOR3D time series are available until 2020, while the MEDREA24 time series is provided
68 up to 2021 (last 6 months extended in interim mode).

69 The salinity anomalies are computed using formula (2). The difference of the salinity, S, with a reference salinity, S_{ref}, is
70 normalised by the depth of the water column which is constant in our case with $z_2 = 300$ m and $z_1 = 0$ m.

$$S_A = \int_{z_1}^{z_2} \frac{S - S_{ref}}{z_2 - z_1} dz$$

71 (2)

73 Formula (2) is a modified version of the one proposed in Boyer et al. (2007) which uses the salinity as a proxy for the
74 equivalent freshwater content. This method has been later adopted in various studies including, among the others, Holliday
75 et al. (2020), with a density weight to account for baroclinic properties of the water column. The formulation in Boyer et al.
76 (2007) is based on a reference salinity. As an example, mean values of a basin (Aagaard and Carmack, 1989) is a widely used
77 choice for S_{ref} in global freshwater content calculations. However, it is argued that since a reference value can be chosen
78 arbitrarily, this would bring ambiguity (Schauer and Losch, 2019) in computing the equivalent freshwater content. Therefore,
79 in this study we propose to evaluate the salinity content and anomaly following formula (2) by choosing S_{ref} as a monthly
80 climatology of each dataset computed from each product separately between 1993 and 2014. This period is chosen to be
81 consistent with the Ocean Monitoring Indicators produced previously in the Mediterranean Sea and other Copernicus Marine
82 domains. Furthermore, the calculations are performed in the entire Mediterranean Sea (MED) as well as in its western
83 (WMED) and eastern (EMED) sub basins, separated at the Sicily Strait. In Fig. 1, we present the monthly variation of the
84 S_{ref}, as an example only the one from MEDREA24, which shows a clear difference in the seasonality in the EMED and
85 WMED, with a maximum in March and December, respectively. It is also evident that the Mediterranean monthly salinity
86 reference shows a seasonal cycle much similar to the one of the Eastern basin (but with different magnitude) characterised
87 by lower salinity during the summer period and larger values at the end of the year.

3 Results and Discussion

The Copernicus Marine service products described in the previous section allow the assessment of the salinity content of the Mediterranean Sea along with its anomaly and trend during the last decades.

In Fig. 2, we present the time series of the mean salinity content in the first 300 m derived from the analysed products (MEDREA24 in red; GREP ensemble mean in blue; GREP ensemble members in thin light blue; CORA in dark green, ARMOR3D in light green) and their overall mean (in black) and spread (shaded grey).

In the early 90s in the entire Mediterranean Sea (Fig. 2a), there is a large spread in salinity with the observations showing a higher salinity while the reanalysis products present relatively lower salinity. This is the case until 2005. Coinciding with the global coverage of the Argo profilers in the early 2000s following the efforts in the Global Ocean Data Assimilation (GODAE) together with the Climate Variability and Predictability Programme (CLIVAR) and the Global Climate Observing System/Global Ocean Observing System (GCOS/GOOS), the spread among different products narrows. Possibly, the reanalyses are better constrained through data assimilation with this novel observation type (Johnson et al., 2022) which provides high-resolution and high-frequency temperature and salinity profiles all over the world' ocean while the observation-based gridded products become more confident. The maximum spread between the period 1993-2019 is in the 90's with a value of 0.096 psu and it decreases to as low as 0.009 psu by the end of 2010s. The mean salinity computed in the entire Mediterranean Sea from all products varies between approximately 38.5 and 38.6 psu with a spatiotemporal mean of 38.57 psu (Table 1).

In the western Mediterranean (Fig. 2b), the overall mean is centred around 38.16 psu with a larger spread - with a maximum and minimum of 0.172 psu and 0.026, respectively - occurring in the early 2000s. An increase of the mean salinity in 2005 is evident from all the reanalysis products and, at a lesser extent, from the CORA dataset, for which one of the many possible reasons is the regime shift as discussed in (Schroeder et al., 2016) corresponding to a major deep water formation event at the beginning of the Western Mediterranean Transition (Zunino et al., 2012).

In the eastern Mediterranean (Fig. 2c), the overall mean is centred around 38.87 psu with a lower spread compared to the western basin with a maximum and minimum of 0.086 psu and 0.003, respectively.

Overall, for the period between 1993-2019 we note that the observational products, gridded using optimal interpolation statistical techniques, show a higher average salinity compared to the reanalysis products that are dynamically integrated and corrected through data assimilation. The spread is representing the offset of the products more than their variability in the entire Mediterranean Sea, as well as in its eastern and western subdomains.

All the products show a positive trend between 1993-2019 (in parenthesis in Table 1). The trend in the mean of all products is calculated as 0.0056 psu/year. This trend is consistent with the estimates between 1950-2002 of Skliris et al., (2018) from EN4 and MEDATLAS data sets which shows a trend of 0.0096 ± 0.0077 and 0.0088 ± 0.0092 respectively, in the first 150

119   m while 0.0067 ± 0.0040 and 0.0067 ± 0.0036 between 150-600 m. The trend calculated for each grid point from the

120   MEDREA24, which is the analysed product covering the longest period, is presented in Fig. 2d. The dominant signal in the

121   entire basin is positive with a larger amplitude in the Balearic Sea, Ionian Sea, Adriatic Sea, Western Levantine and with a

122   less evident signal in the Gulf of Lions, Northern Aegean Sea and Eastern Levantine Basin. A small negative trend zone

123   appears in the Alboran Sea. The trend in the entire analysed period is about 0.0049 psu/year in the western basin. This is

124   below the rate of the basin-wide trend which is larger due to the trend in the eastern basin (0.0061 psu/yr).

125

126   For 2020, CORA and ARMOR3D products are available, and both continue to sustain the positive trend even though it is

127   less evident in the western basin. MEDREA24 (and its interim extension) shows an increasing mean salinity until the end of

128   2021. All products present larger values after 2016 and a maximum in 2018.

129   The spatial mean, computed between 1993-2014 from all products in the first 300 m (Fig. 3a), shows a gradual increase in

130   the upper ocean integrated salinity from west to east. Minimum salinity occurs close to river mouths, such as in the North

131   Adriatic Sea due to the freshwater input from the Po River, and on the pathways of the outflow of the Dardanelles and

132   Gibraltar straits. The Atlantic water, modified through its route, can be traced till the eastern basin from its low salinity. The

133   spread deduced from all the products (Fig. 3b) implies that they agree more, meaning lower spread, in the Levantine and

134   Ionian Seas and to a lesser degree between the Balearic and Sardinia / Corsica islands. The spread is larger especially in the

135   northern Aegean and Adriatic Sea and southwestern coast between the Gulf of Gabes and Gibraltar Strait. This uncertainty

136   or mismatch in the products is possibly due to the different volume fluxes through the rivers and straits.

137   In Fig. 4 (a-c), we show the time series of the salinity anomaly estimates in the western (Fig. 4a), eastern (Fig. 4b) and entire

138   (Fig. 4c) basin from each product using formula (2). We recall that the salinity reference is computed for each product per

139   se. Moreover, the salinity anomaly map in 2021 from MEDREA24 is depicted in Fig. (4d), computed against the overall

140   mean between 1993-2014, which is shown in Fig. (3a).

141   The anomalies have a larger range in the reanalysis products. There is a negative anomaly within the first decade in GREP

142   and MEDREA24 which turns to positive first in the western Mediterranean (Fig. 4a) and followed by the eastern basin (Fig.

143   4b) after 2006. In the CORA and ARMOR3D, instead, there is a clear increase in the salinity anomaly in the eastern

144   Mediterranean and the entire basin with a less evident positive trend in the western basin. We summarise the mean salinity

145   anomalies in Table 2.

146   In 2021, the anomaly is mostly positive with some negative anomaly structures on the path of Atlantic water (Fig. 4d),

147   Alboran Sea, upwelling favouring Balearic Islands. Fedele et al. (2022) reports a positive salinity trend in the modified

148   Atlantic and Levantine intermediate waters using 18-year long (2001-2019) Argo profiles, which in general agrees with the

149   anomaly map to a large extent. However, we note that the spread on the pathway of the water entering from the Gibraltar

150   strait and reaching the Levantine basin has a relatively larger spread compared to the deeper areas (see Fig. 3b).

4 Conclusions

In this study, we presented the salinity characteristics of the Mediterranean Sea in the upper 300 m deduced from various products including reanalysis and gridded observational datasets released by Copernicus Marine Service. The products with dynamically constructed ocean reanalysis and objectively analysed observations show significantly large spread at the beginning of the period of investigation while the uncertainty reduces possibly with the emergence of ARGO profilers which allowed a wider spatial and higher frequency sampling in the ocean. The mean salinity with its anomaly and trend is computed and analysed in the entire basin as well as in the western and eastern basins for all the datasets separately and averaged. The spatial maps of the mean and the spread of the salinity are depicted and discussed. The overall results show a salinification of the Mediterranean Sea agreeing with earlier studies (e.g., Skliris et al. 2018). The subbasin scale investigation shows negative salinity anomalies in the western basin in the upwelling regions, which may imply stronger upwelling events, and waterway following the north African coast, which may be a consequence of the freshening North Atlantic water masses (Holliday et al., 2020). There is a large spread in the salinity estimates among different products, which reduces with the introduction of the Argo profilers in the data assimilation components of the reanalysis systems. Besides the large spread, considering the reported discrepancies in the salinity measurements after 2016 (Barnoud et al., 2021), it is essential to use all available information sources for a more accurate state estimate and uncertainty quantification.

Data availability

All datasets used in this article can be obtained from the Copernicus Marine Service catalogues as described in Table 3 with their names, temporal coverages, and documentation.

Acknowledgments

This study has been conducted using EU Copernicus Marine Service Information. This work has been funded through the EU Copernicus Marine Med-MFC Service Lot n. 21002L5-COP-MFC MED-5500.

References

Aagaard, K., and Carmack, E. C.: The role of sea ice and other fresh water in the Arctic circulation. *Journal of Geophysical Research: Oceans*, *94*(C10), 14485-14498. 1989.

Aydoğdu, A., Pinardi, N., Özsoy, E., Danabasoglu, G., Gürses, Ö., and Karspeck, A.: Circulation of the Turkish Straits System under interannual atmospheric forcing. *Ocean Science*, *14*(5), 999-1019. 2018.

Barnoud, A., Pfeffer, J., Guérou, A., Frery, M.-L., Siméon, M., Cazenave, A., et al.: Contributions of altimetry and Argo to non-closure of the global mean sea level budget since 2016. Geophysical Research Letters, 48, e2021GL092824. https://doi.org/10.1029/2021GL092824, 2021.

Blockley, E. W., Martin, M. J., McLaren, A. J., Ryan, A. G., Waters, J., Lea, D. J., ... and Storkey, D.: Recent development of the Met Office operational ocean forecasting system: an overview and assessment of the new Global FOAM forecasts. *Geoscientific Model Development*, 7(6), 2613-2638. 2014.

Boyer, T., Levitus, S., Antonov, J., Locarnini, R., Mishonov, A., Garcia, H., and Josey, S. A.: Changes in freshwater content in the North Atlantic Ocean 1955–2006. *Geophysical Research Letters*, *34*(16). 2007.

Bretherton, F. P., R. E. Davis and C. B. Fandry, A technique for objective analysis and design of oceanographic experiments applied to MODE-73, 1976 / Deep-Sea Res., 23, 559-582

Cessi, P., Pinardi, N., and Lyubartsev, V.: Energetics of semienclosed basins with two-layer flows at the strait. *Journal of physical oceanography*, *44*(3), 967-979. 2014.

Cheng, L., Trenberth, K. E., Gruber, N., Abraham, J. P., Fasullo, J. T., Li, G., Mann, M. E., Zhao, X., and Zhu, J.: Improved Estimates of Changes in Upper Ocean Salinity and the Hydrological Cycle, *Journal of Climate*, *33*(23), 10357-10381. doi: 10.1175/J9-2022, 2022.CLI-D-20-0366.1, 2020.

Cos, J., Doblas-Reyes, F., Jury, M., Marcos, R., Bretonnière, P.A., and Samsó, M.: The Mediterranean climate change hotspot in the CMIP5 and CMIP6 projections, Earth Syst. Dynam., 13, 321–340, https://doi.org/10.5194/esd-13-321-2022, 2022.

Dayan, H., McAdam, R., Masina, S., and Speich, S.: Diversity of marine heatwave trends across the Mediterranean Sea over the last decades, in: Copernicus marine service ocean state report, issue 6, Journal of Operational Oceanography, vol. 15, pp. 49–56, 2022.

Fedele, G., Mauri, E., Notarstefano, G., and Poulain, P. M.: Characterization of the Atlantic Water and Levantine Intermediate Water in the Mediterranean Sea using 20 years of Argo data, Ocean Sci., 18, 129–142, https://doi.org/10.5194/os-18-129-2022 , 2022.

Escudier, R., Clementi, E., Cipollone, A., Pistoia, J., Drudi, M., Grandi, A., Lyubartsev, V., Lecci, R., Aydogdu, A., Delrosso, D., Omar, M., Masina, S., Coppini, G., and Pinardi, N. (2021) A High Resolution Reanalysis for the Mediterranean Sea. Front. Earth Sci. 9:702285. doi: 10.3389/feart.2021.702285, 2021.

Guinehut, S., Dhomps, A-L., Larnicol, G., Le Traon, P-Y.: High resolution 3D temperature and salinity fields derived from in situ and satellite observations. Ocean Sci 8:845–857. doi:10.5194/os-8-845-2012, 2012.

205 Holliday, N.P., Bersch, M., Berx, B., Chafik, L., Cunningham, S., Florindo-López, C., Hátún, H., Johns, W, Josey, SA.,
206 Larsen, K.M., Mulet, S.: Ocean circulation causes the largest freshening event for 120 years in eastern subpolar North
207 Atlantic. *Nat Commun* **11,** 585. https://doi.org/10.1038/s41467-020-14474-y, 2020.

208 Jarosz, E., Teague, W. J., Book, J. W., & Beşiktepe, Ş. T. (2013). Observed volume fluxes and mixing in the Dardanelles
209 Strait. Journal of Geophysical Research: Oceans, 118(10), 5007-5021.

210 Johnson G. C., Hosoda S., Jayne S. R., Oke P. R., Riser S. C., Roemmich D., Suga T., Thierry V., Wijffels S. E. and Xu, J.:
211 Argo-two decades: global oceanography, revolutionized. *Annual review of marine science*, *14*, 379-403. 2022.

212 Jordà, G., Von Schuckmann, K., Josey, S. A., Caniaux, G., García-Lafuente, J., Sammartino, S., Özsoy E, Polcher J,
213 Notarstefano G, Poulain PM, Adloff F., Salat J., Naranjo C., Schroeder K., Chiggiato J., Sannino G., and Macías, D.: The
214 Mediterranean Sea heat and mass budgets: Estimates, uncertainties and perspectives. Progress in Oceanography, 156, 174-
215 208. https://doi.org/10.1016/j.pocean.2017.07.001, 2017.

216 Juza, M, Fernández-Mora, À, and Tintoré, J.: Sub-Regional Marine Heat Waves in the Mediterranean Sea From Observations:
217 Long-Term Surface Changes, Sub-Surface and Coastal Responses. *Front. Mar. Sci.* 9:785771. doi:
218 10.3389/fmars.2022.785771, 2022.

219 Lellouche, J. M., Le Galloudec, O., Drévillon, M., Régnier, C., Greiner, E., Garric, G., ... and De Nicola, C.: Evaluation of
220 global monitoring and forecasting systems at Mercator Océan. *Ocean Science*, *9*(1), 57-81. 2013.

221 Pisano, A., Marullo, S., Artale, V., Falcini, F., Yang, C., Leonelli FE, Santoleri, R., and Buongiorno Nardelli, B.: New
222 Evidence of Mediterranean Climate Change and Variability from Sea Surface Temperature Observations. Remote Sensing.
223 12(1):132. https://doi.org/10.3390/rs12010132, 2020.

224 Sannino, G., Sözer, A., and Özsoy, E.: A high-resolution modelling study of the Turkish Straits System. *Ocean Dynamics*,
225 *67*(3), 397-432. 2017.

226 Schauer, U., and Losch, M.: "Freshwater" in the ocean is not a useful parameter in climate research. *Journal of Physical*
227 *Oceanography*, *49*(9), 2309-2321. 2019.

228 Schroeder, K., Chiggiato, J., Bryden, H. L., Borghini, M., and Ben Ismail, S.: Abrupt climate shift in the Western
229 Mediterranean Sea. *Scientific reports*, *6*(1), 1-7. 2016.

230 Skliris, N., Zika, J. D., Herold, L., Josey, S. A., and Marsh, R.: Mediterranean sea water budget long-term trend inferred from
231 salinity observations. Climate Dynamics, 51(7), 2857-2876. https://doi.org/10.1007/s00382-017-4053-7, 2018.

232 Soto-Navarro, J., Criado-Aldeanueva, F., García-Lafuente, J., & Sánchez-Román, A. (2010). Estimation of the Atlantic
233 inflow through the Strait of Gibraltar from climatological and in situ data. Journal of Geophysical Research: Oceans,
234 115(C10).

235 Storto, A., Masina, S. and Navarra, A.: Evaluation of the CMCC eddy-permitting global ocean physical reanalysis system
236 (C-GLORS, 1982–2012) and its assimilation components. Q.J.R. Meteorol. Soc., 142: 738–758. doi:10.1002/qj.2673, 2016.

237 Storto, A., Masina, S., Simoncelli, S. et al.: The added value of the multi-system spread information for ocean heat content
238 and steric sea level investigations in the CMEMS GREP ensemble reanalysis product. Clim Dyn 53, 287–312.
239 https://doi.org/10.1007/s00382-018-4585-5, 2019a.

240 Storto, A., Alvera-Azcárate, A., Balmaseda, M. A., Barth, A., Chevallier, M., Counillon, F., ... and Zuo, H.: Ocean reanalyses:
241 recent advances and unsolved challenges. *Frontiers in Marine Science*, 6, 418. 2019b.

242 Szekely, T., Gourrion, J., Pouliquen, S., and Reverdin, G.: The CORA 5.2 dataset for global in situ temperature and salinity
243 measurements: data description and validation, Ocean Sci., 15, 1601–1614, https://doi.org/10.5194/os-15-1601-2019, 2019.

244 Tuel, A., and Eltahir, E. A. B.: Why Is the Mediterranean a Climate Change Hot Spot?, Journal of Climate, 33(14), 5829-
245 5843. Retrieved Jan 25, 2022, from https://journals.ametsoc.org/view/journals/clim/33/14/JCLI-D-19-0910.1.xml, 2020.

246 Zunino, P., Schroeder, K., Vargas-Yáñez, M., Gasparini, G. P., Coppola, L., García-Martínez, M. C. and Moya-Ruiz, F.:
247 Effects of the Western Mediterranean Transition on the resident water masses: Pure warming, pure freshening and pure
248 heaving. Journal of Marine Systems 15, 96–97. doi: 10.1016/j.jmarsys.2012.01.011, 2012.

249 Zuo, H., Balmaseda, M. A., and Mogensen, K.: The new eddy-permitting ORAP5 ocean reanalysis: description, evaluation
250 and uncertainties in climate signals. Clim. Dyn. 49, 791–811. doi: 10.1007/s00382-015-2675-1, 2017.
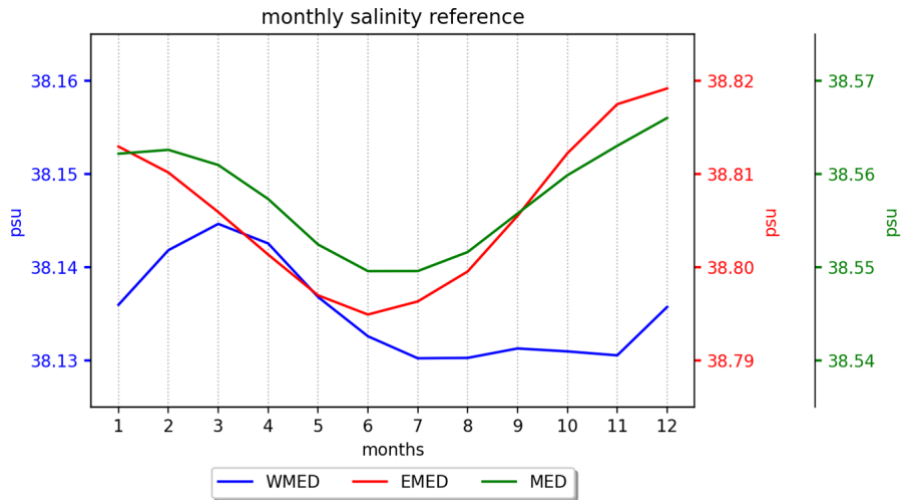
251

252 **Figure 1:** The monthly reference salinity S_{ref} estimates calculated from the MEDREA24 in the period 1993-2014. The green,
253 blue, and red curves show the MED, WMED and EMED regions respectively on its corresponding vertical axis. The same
254 calculation is done for each product separately (not shown) to evaluate formula (2) to compute salinity anomaly.

255

psu (psu/year)	MED	WMED	EMED
MEDREA24	38.58 (0.0070)	38.15 (0.0055)	38.83 (0.0078)
GREP	38.48 (0.0110)	38.01 (0.0111)	38.87(0.0106)
CORA	38.61 (0.0020)	38.21(0.0019)	38.84 (0.0024)
ARMOR3D	38.64 (0.0027)	38.24 (0.0020)	38.75(0.0032)
mean	38.57 (0.0056)	38.16 (0.0049)	38.87 (0.0061)

256   **Table 1.** The temporal mean salinity (in psu) and trend (in psu per year) in the 0-300 m between the common period 1993-

257   2019 for separate products and their overall mean in *Fig. 2*.
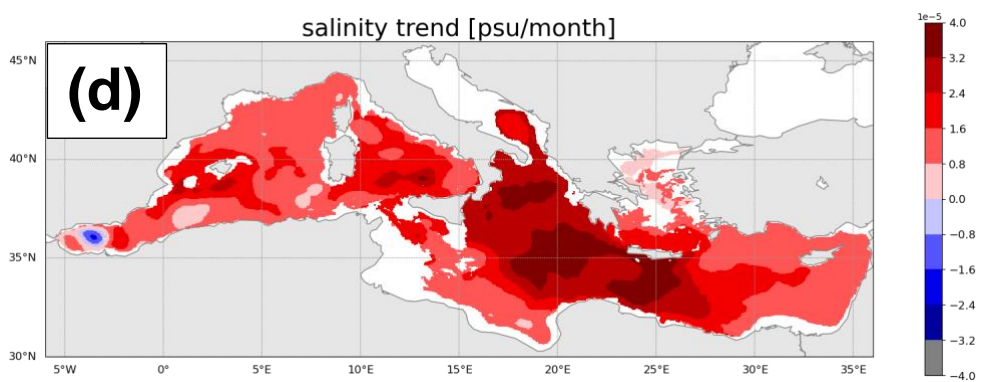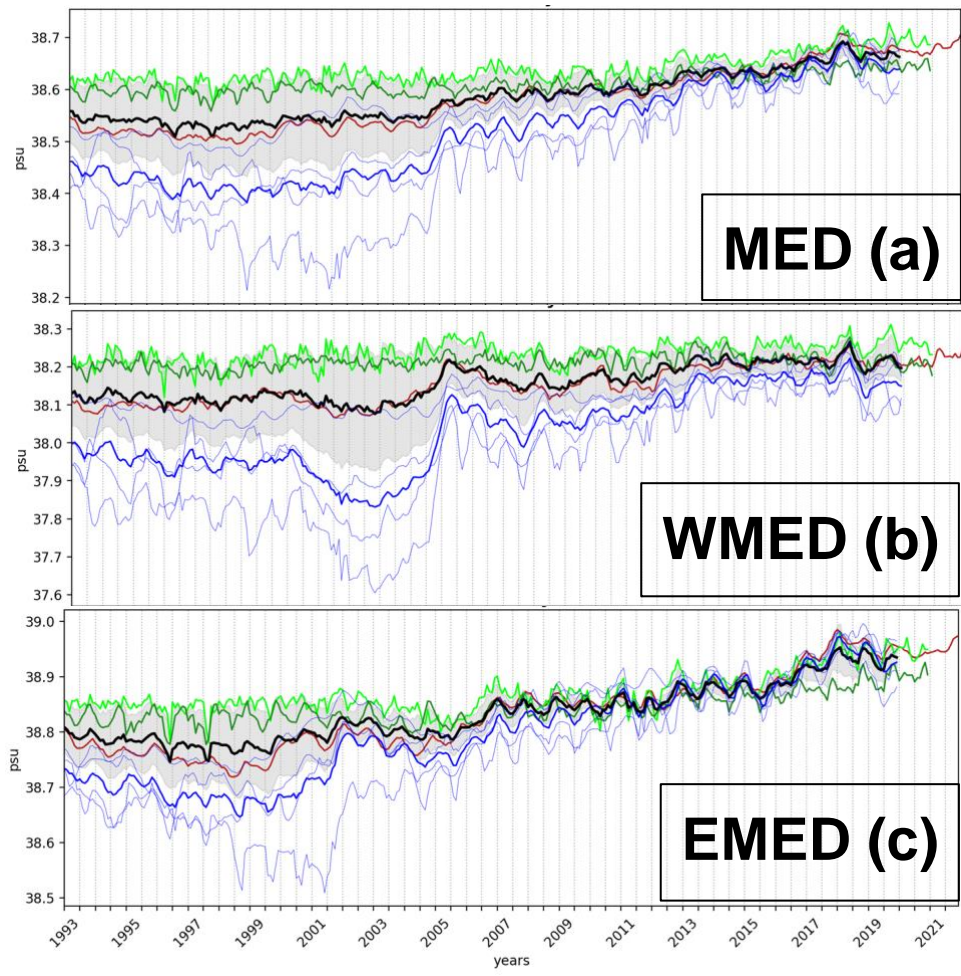
Figure 2: Time series of mean salinity in the upper 300 m in the **(a)** entire Mediterranean Sea **(b)** western Mediterranean basin and **(c)** eastern Mediterranean basin between the period 1993 and 2021 from MEDREA24, until the end of 2020 for ARMOR3D, CORA and until the end of 2019 for GREP. The mean of all the products is drawn in black with their standard deviation shaded around the mean. GREP ensemble members are depicted in thin blue curves. The GREP product covers the period until 2019 while the observational products CORA and ARMOR3D cover until 2020. The time series for MEDREA24 is extended until 2021 using the interim products. (d) salinity in the first 300 m. from the MEDREA24.
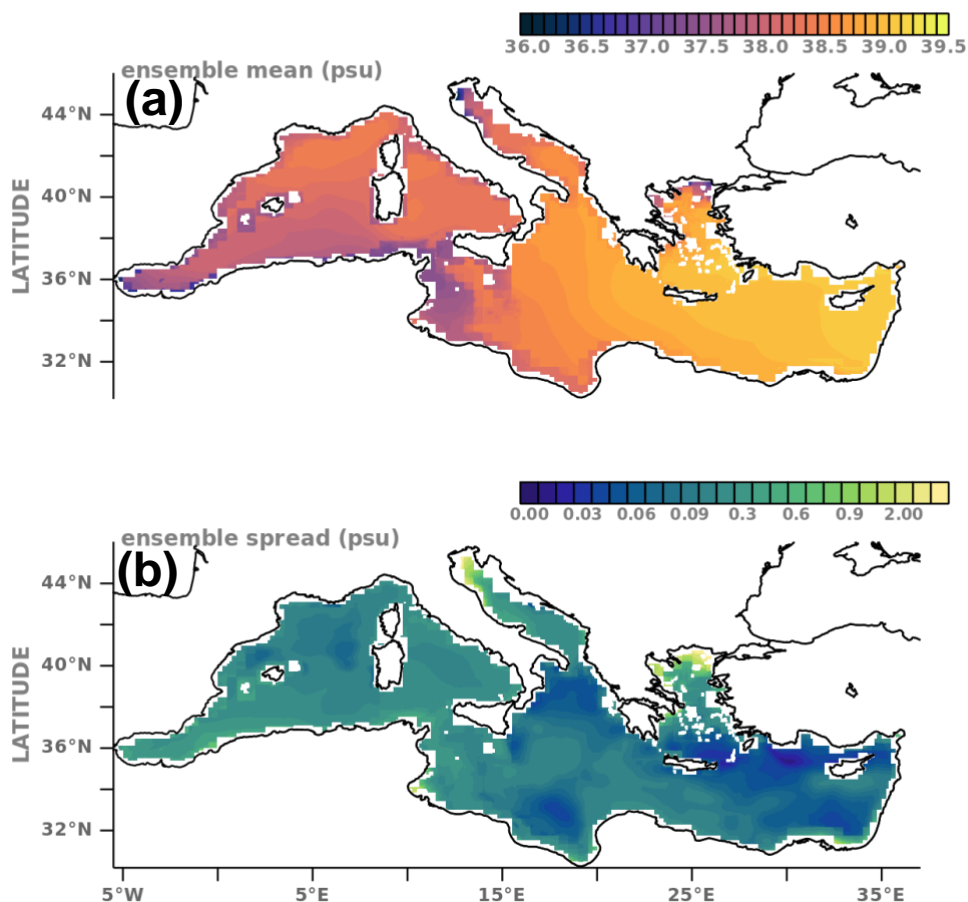
Figure 3. The maps of **(a)** mean and **(b)** spread of integrated salinity in the period between 1993–2014 in 0-300 m. computed from the GREP ensemble mean, CORA, ARMOR3D and MEDREA24 products. We refer to the text for the information on the data products used. The analysis is performed only if the water column is deeper than 300 m. Note that in **(b)** the colour scale is not linear to show the smaller standard deviation.

270

psu	MED	WMED	EMED
MEDREA24	0.026	0.027	0.025
GREP	0.042	0.056	0.034
CORA	0.001	-0.008	0.007
ARMOR3D	0.001	-0.009	0.008
mean	0.018	0.017	0.019

Table 2. The temporal mean salinity anomaly (in psu) in the 0-300 m between the common period 1993-2019 for separate products and their average in *Fig. 3*.

273

274
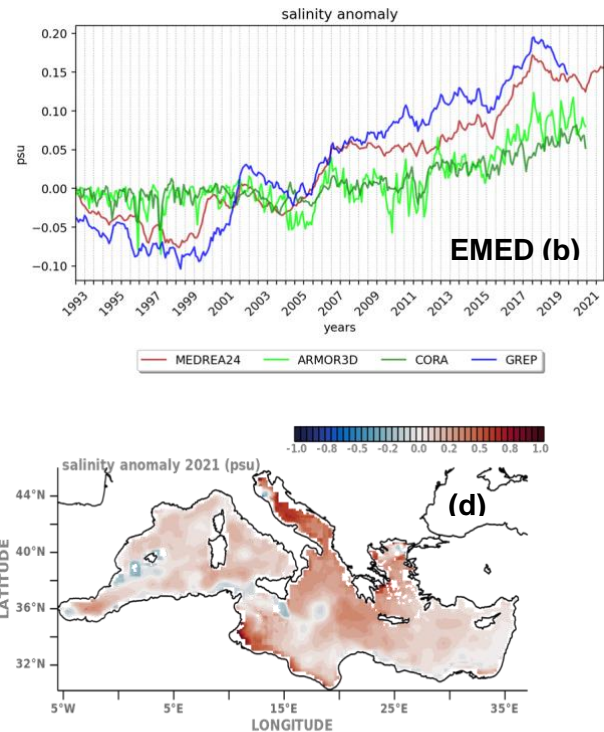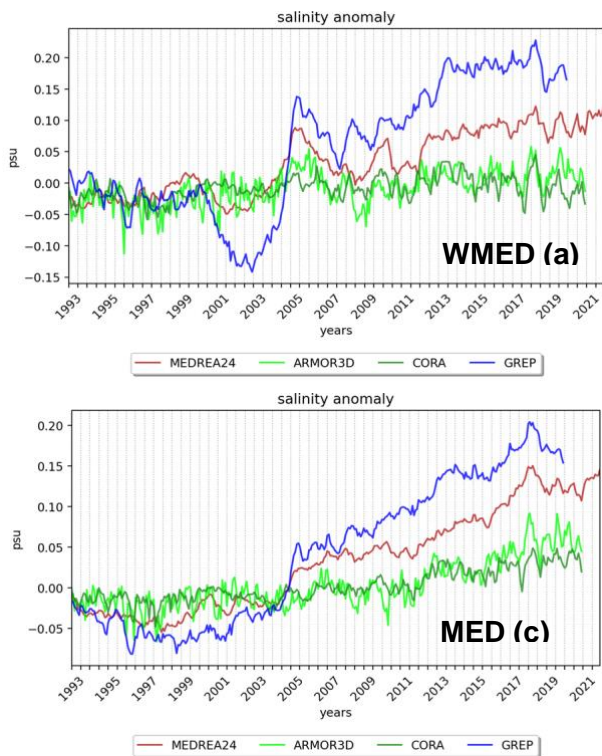
Figure 4. Time series of salinity anomaly from the MEDREA24, GREP, ARMOR3D and CORA products in the **(a)** western Mediterranean Sea **(b)** eastern Mediterranean basin and **(c)** entire Mediterranean basin computed with respect to the monthly reference salinity estimates in the corresponding area in **Fig. 1** calculated from the MEDREA24 in the period 1993-2014. The GREP products cover the period until 2019 while the observational products CORA and ARMOR3D covers until 2020. The time series for MEDREA24 is extended until 2021 using the interim products. **(d)** salinity anomaly in 2021 in the Mediterranean Sea against the mean of salinity in Fig. 3a.

	Product Name	Documentation	Time Period
Mediterranean Sea Physics Reanalysis	MEDSEA_MULTIYEAR_PHY_006_004	Product User Manual (CMEMS-MED-PUM-006-004) Quality Information Document (CMEMS-MED-QUID-006-004) https://resources.marine.copernicus.eu/product-detail/MEDSEA_MULTIYEAR_PHY_006_004/DOCUMENTATION	1987-2021
Global Ocean Ensemble Physics Reanalysis	GLOBAL_REANALYSIS_PHY_001_031	Product User Manual (CMEMS-GLO-PUM-001-031) Quality Information Document (CMEMS-GLO-QUID-001-031) https://resources.marine.copernicus.eu/product-detail/GLOBAL_REANALYSIS_PHY_001_031/DOCUMENTATION	1993-2019

Global Ocean-Delayed Mode gridded CORA-In-situ Observations objective analysis in Delayed Mode	INSITU_GLO_TS_OA_REP_OBSERVATIONS_013_002_b	Product User Manual (CMEMS-INS-PUM-013-002-ab) Quality Information Document (CMEMS-INS-QUID-013-002b) https://resources.marine.copernicus.eu/product-detail/INSITU_GLO_TS_OA_REP_OBSERVATIONS_013_002_b/DOCUMENTATION	1993-2020
Multi Observation Global Ocean 3D Temperature Salinity Height Geostrophic Current and MLD	MULTIOBS_GLO_PHY_TSUV_3D_MYNRT_015_012	Product User Manual (CMEMS-MOB-PUM-015-012) Quality Information Document (CMEMS-MOB-QUID-015-012) https://resources.marine.copernicus.eu/product-detail/MULTIOBS_GLO_PHY_TSUV_3D_MYNRT_015_012/DOCUMENTATION	1993-2020

281   **Table 3.** Products from Copernicus Marine Service used in this study.